Scattering in the Atmosphere of Venus. III.

Line Profiles and Phase Curves for Rayleigh Scattering

by

L. D. G. Young and George W. Kattawar
Department of Physics
Texas A&M University
College Station, Texas 77843

Report No. 25

The research described in this report was funded by the

National Aeronautics and Space Administration

Contract No. NGR-44-001-117

Department of Physics
Texas A&M University
College Station, Texas 77843

March 17, 1976

A paper based on the material in this report has been submitted to Icarus.

(NASA-CR-146535) SCATTERING IN THE ATMOSPHERE OF VENUS. LINE PROFILES AND PHASE CURVES FOR RAYLEIGH SCATTERING (Texas A&M Univ.) 21 p HC $3.50 CSCL 03B

N76-21100

Unclas

G3/91 20730

Scattering in the Atmosphere of Venus III

Line Profiles and Phase Curves for Rayleigh Scattering

by

L. D. G. Young and George W. Kattawar

Department of Physics

Texas A&M University

College Station, Texas 77843

Abstract

Spectral line profiles, curves of growth and curves for the equivalent width of a line as a function of Venus phase angle have been computed for a Rayleigh scattering cloud and compared with those for a cloud of isotropic scatterers. The results are very similar for the two kinds of scattering, with the exception for the curves of equivalent width as a function of Venus phase angle. These latter curves exhibit the "inverse phase effect" and rule out the possibility that the scale height of the clouds can be much less than half the scale height of the gas. The optical depth of the clouds is approximately τ_c=100.

1. Introduction

In our previous papers of this series (Young and Kattawar, 1976, hereafter called Part I; Kattawar and Young 1976, hereafter called Part II) we assumed that the clouds scattered radiation isotropically. We examined the effects of varying the scattering optical thickness of the clouds on the curve of growth. In Part I, we assumed an inhomogeneous model atmosphere, at a constant temperature, with pressure decreasing as the height above the surface of the planet increases. The calculations were made for a 4-layer atmosphere with the cloud "bottom" at a pressure of two bars. The Curtis-Godson approximation was shown to be applicable for transmitted radiation even in the case of multiple scattering. An error of only 3% was caused by the replacement of a 4-layer atmosphere with a single layer even for scattering optical depths as large as τ_C=100. We found that the curves of growth always had the limiting slopes of one (for weak absorption) and 0.5 (for strong absorption), as is the case for a curve of growth measured for a non-scattering atmosphere.

In Part 1 we also computed curves of growth for different angles of incidence and reflection as well as for the radiation integrated over the visible disk. The curves were parallel to one another, with the curves for large Venus phase angles lying below the curve for $i=0^o$ phase. By comparing the computed variation of the equivalent width, W, of an absorption line with Venus phase angle with the observed variation, we concluded that the optical depth of the clouds had to be $\tau_C \geq 10$.

In Part II, again assuming isotropic scattering, we examined the effects of allowing the temperature of the gas to vary in the atmosphere. We found that this did not drastically change the shape of the curve for relative

equivalent width versus Venus phase angle. We also allowed the scale height of the cloud particles to vary relative to the scale height of the gas. This produced a very marked change in the variation of equivalent width with Venus phase angle. It permitted us to rule out the possibility that the cloud optical depth was much less than τ_c=100, or that the scale height of the cloud, H_c, could be as small as one-third of the scale height of the gas, H_g.

All of the above conclusions were based on the assumption that the cloud particles scatter isotropically. We know that this is not the situation for the clouds of Venus. In this paper we will examine the effect of a slightly anisotropic scattering function, namely Rayleigh scattering. There have been various theoretical calculations made for Rayleigh scattering, but usually for a homogeneous atmosphere. We will again use a 4-layer model atmosphere, with the temperature and pressures of the layers corresponding to Marov's model of the Venus atmosphere.

2. Calculation of line profiles for reflected radiation

In Figures 1 through 3 we show the computed line profiles for Rayleigh scattering and for isotropic scattering. For these calculations we have assumed the cloud scale height, H_c, to be equal to the scale height of the gas, Hg, the optical thickness of the cloud, τ_c = 100 which gives a computed Bond albedo A_B=0.896, and the abundance, w, line strength, S_L, product for the CO_2 lines to be $wS_L = 9.18 \times 10^{-2}$ cm^{-1}. (This corresponds to a typical line in the 8689Å CO_2 band). Figure 1 is for a Venus phase angle of $i=0^0$, Figure 2 is for $i=80^0$ and Figure 3 is for $i=140^0$. One thing is immediately apparent: It would be almost impossible to distinguish between isotropic and Rayleigh scattering on the basis of observed line profiles. The least amount of noise in the data (which is always present) would make the two similar line profiles very hard to tell apart except at the line center. In practice, the instrumental slit function degrades the line profile and this would tend to make the line shapes even more similar in appearance. It should also be noted that for $i=0^0$ the line for isotropic scattering lies below that for Rayeligh scattering, while at 80^0 the situation is reversed, and at $i=140^0$ it is reversed again. This effect is brought out further by considering Table 1. Here we show absolute equivalent widths for both Rayleigh and isotropic scattering particles relative to the gas. Much of this behavior can be explained by considering the single scattering phase functions. For scattering angles between 55^0 and 125^0 the Rayleigh phase function lies below the isotropic and for angles less that 55^0 and greater than 125^0 the opposite is true. Therefore, from a single scattering analysis alone one would expect less absorption,

hence a smaller equivalent width, for Rayeligh scattering near inferior and superior conjunctions with the opposite behavior occuring for phase angles between 55^o and 125^o. This is precisely what the data in Table 1 show. This general behavior is also independent of the scale height of the particles. From this analysis we can infer what will happen with more anisotropic phase functions. In general they will have equivalent widths larger than the isotropic case near superior conjunction and smaller than the Rayleigh case near inferior conjuction.

3. Calculation of the Variation of the Equivalent width of a CO_2 line with Venus Phase Angle

Figure 4 gives a comparison of the phase variation for 3 carbon dioxide lines which vary in line strength; the maximum range in line strengths is a factor of 10^3, corresponding to the range of the strengths for the CO_2 bands observed in the photographic infrared. The three curves for isotropic scattering exhibit a monotonic decrease with increasing Venus phase angle. The three curves for Rayleigh scattering exhibit an increase in equivalent width between $0^o \leq i \leq 60^o$ and then a decrease for increasing values of the phase angle, with the curves for the weaker lines decreasing more rapidly than the curve for the strongest line. In principle, then, we can see the difference in the phase curves for isotropic and Rayleigh scattering. In practice; the day-to-day variation of equivalent widths (for lines formed in the atmosphere of Venus) is larger than the effect produced by the two types of scattering. The general run of the observations suggest that they are better fit by the curve for Rayleigh scattering than for isotropic scattering. Of course, we know from measurements of the polarization of light reflected from the atmosphere of Venus, that the cloud particles are actually Mie scatterers.

In Fig. 5 we compare curves of growth for Rayleigh and isotropic scattering for the case where $H_c=H_g$ for three diffent phase angles. As can be seen the curves are extremely close together and parallel. They both exhibit the linear weak-line region and the square root strong- line region.

4. Effect of varying the scale height of the scattering particles relative to the scale height of the absorbing gas

Figures 6 through 9 illustrate the effect of varying the scale height of the clouds for both isotropic and Rayleigh scattering. For all four figures a cloud optical thickness of τ_c=100, and an abundance-line strength product of wS_L = 9.18 x 10^{-2} cm^{-1} were used. For both types of scattering. there is a general tendency of the curves to "flatten-out" as H_c decreases from H_g to $H_g/3$. Once again, it appears that the cloud scale height must be larger than $H_g/3$ in order to match the observed curves for Venus. One further thing to note is that the "inverse phase effect" does not require a layer of clear atmosphere between two cloud decks. This confirms the results obtained, using a homogeneous model atmosphere, (Whitehill and Hansen, 1973) and an inhomogenous model atmosphere (Regas, et. al, 1973).

5. Discussion

The general conclusions we arrived at using an istropic scattering model atmosphere, and disccsed in the Introduction, have not changed substantially if a Rayleigh scattering model atmosphere is used. The optical thickness of the clouds must be about $\tau_c = 100$ and the scale height of the clouds must be $H_c > H_g/3$. It should also be clear now that any phase function which is not monotonic at large scattering angles will produce the so called "inverse phase effect."

List of Figures

PAGE BLANK NOT FILMED

Table 1

A comparison of equivalent width versus phase between Rayleigh and Isotropic models. W_R and W_I denote absolute equivalent width in cm^{-1} for Rayleigh and isotropic respectively.

	$H_c=H_g$		$H_c=H_g/3$		$H_c=2H_g$	
Phase Angle (Degrees)	$W_R \times 10^2$ (cm^{-1})	$W_I \times 10^2$ (cm^{-1})	$W_R \times 10^2$ (cm^{-1})	$W_I \times 10^2$ (cm^{-1})	$W_R \times 10^3$ (cm^{-1})	$W_I \times 10^3$ (cm^{-1})
0	1.43	1.56	4.56	4.90	4.31	4.72
30	1.48	1.56	4.71	4.90	4.47	4.71
60	1.51	1.47	4.86	4.76	4.55	4.45
90	1.37	1.28	4.65	4.40	4.12	3.86
120	0.99	0.98	3.89	3.84	2.96	2.93
150	0.50	0.58	2.93	3.15	1.44	1.70

References

G. W. Kattawar and L. D. G. Young (1976) "Scattering in the Atmosphere of Venus II. Effect of Varying the Scale Height of the Scattering Particles," Icarus (in press)

J. L. Regas, R. W. Boese, L. P. Giver and J. H. Miller (1973) "Does spectroscopic evidence require two scattering layers in the Venus atmosphere?" J. Quant. Spectros. Radiat. Transfer 13, 461-463.

L. B. Whitehill and J. E. Hansen (1973) "On the interpretation of the inverse phase effect for CO_2 equivalent width on Venus" Icarus 20 146-152.

L. D. G. Young and G. W. Kattawar (1976) "Scattering in the Atmosphere of Venus I. Line Profiles and Curves of Growth for isotropic scattering" Icarus (in press)

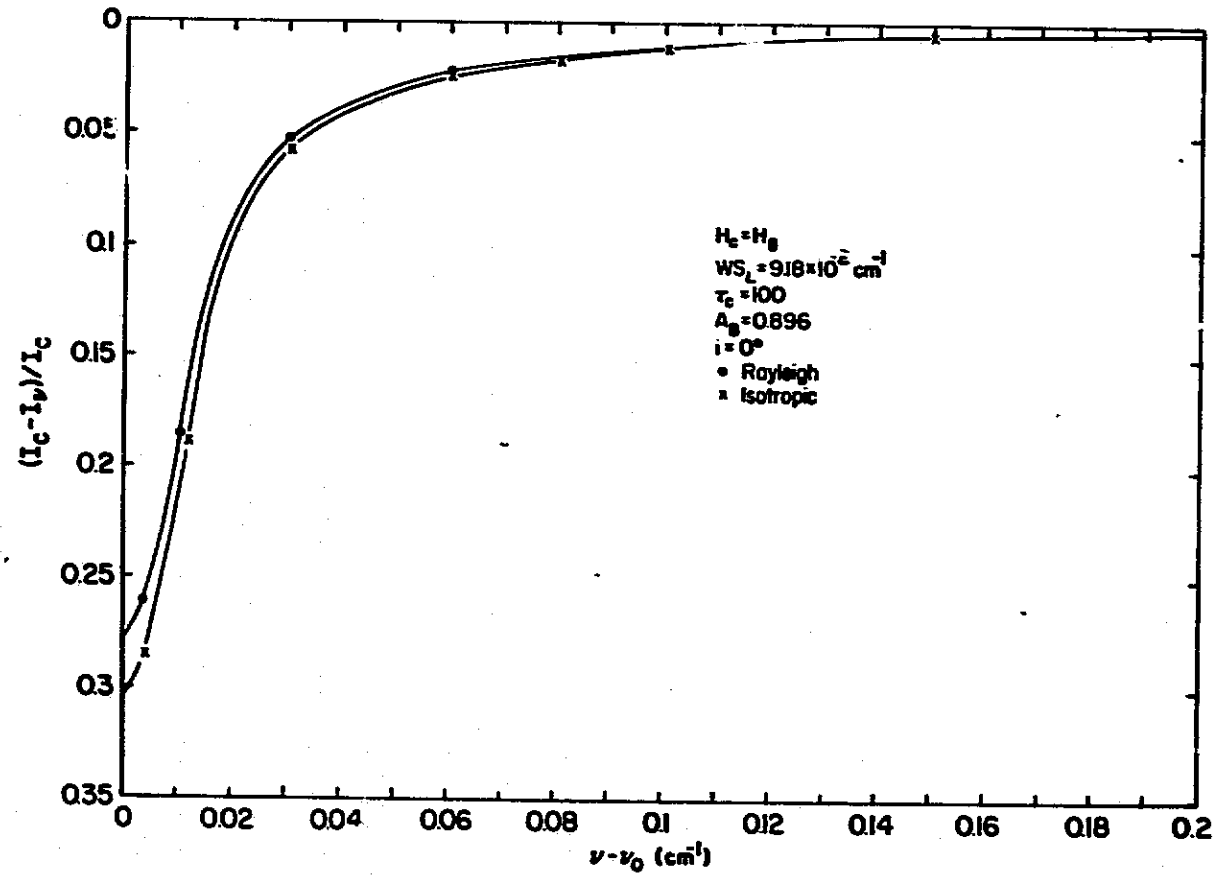
0
0.05
0.1
0.15
0.2
0.25
0.3
0.35
0
0.02
0.04
0.06
0.08
0.1
0.12
0.14
0.16
0.18
0.2
(Ic-Iν)/Ic
ν-ν0 (cm-1)
Hc=HB
WSL=9.18×10-2 cm-1
τc=100
AB=0.896
i=0°
• Rayleigh
x Isotropic

Fig. 1

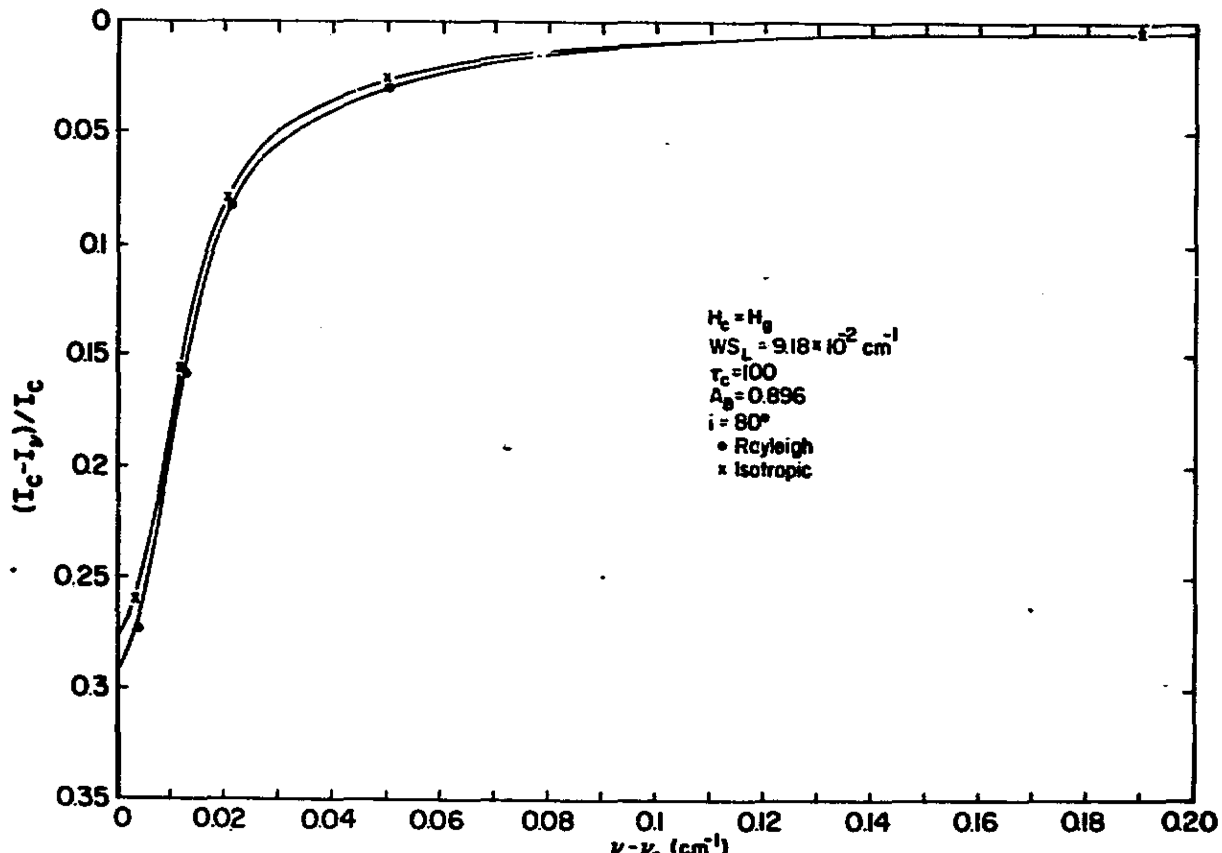
0
0.05
0.1
0.15
0.2
0.25
0.3
0.35
$(I_c-I_\nu)/I_c$
0
0.02
0.04
0.06
0.08
0.1
0.12
0.14
0.16
0.18
0.20
$\nu-\nu_0$ (cm^{-1})
$H_c = H_g$
$WS_L = 9.18 \times 10^{-2}$ cm^{-1}
$\tau_c = 100$
$A_g = 0.896$
$i = 80°$
• Rayleigh
x Isotropic

Fig. 2

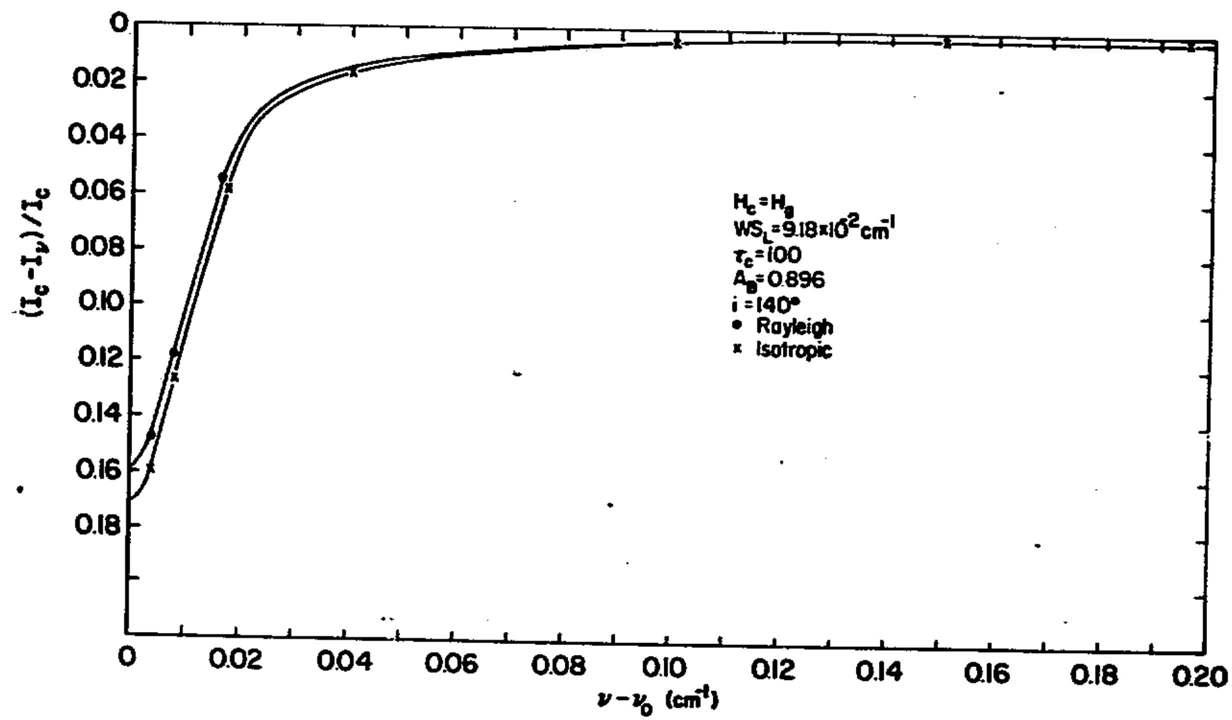
$H_c = H_g$
$WS_L = 9.18 \times 10^{-2}\ cm^{-1}$
$\tau_c = 100$
$A_g = 0.896$
$i = 140°$
• Rayleigh
× Isotropic
$(I_c - I_\nu)/I_c$
$\nu - \nu_0\ (cm^{-1})$
0
0.02
0.04
0.06
0.08
0.10
0.12
0.14
0.16
0.18
0.20

Fig. 3

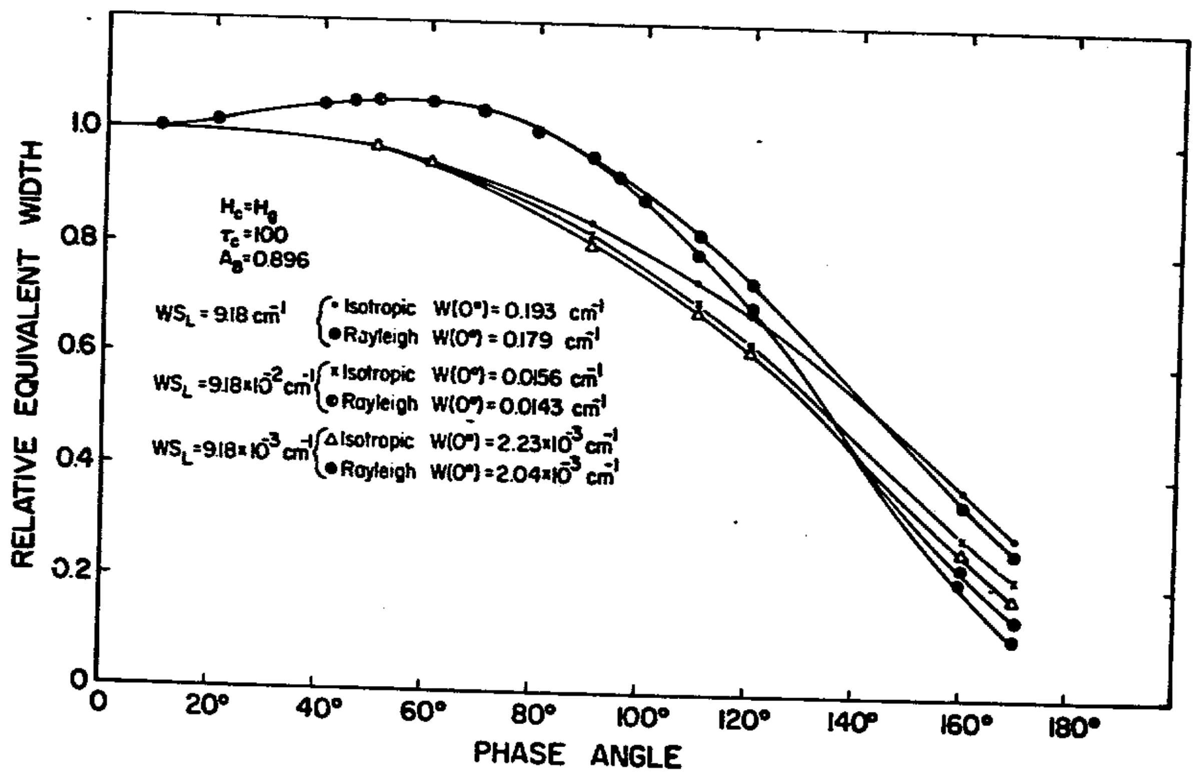
RELATIVE EQUIVALENT WIDTH
1.0
0.8
0.6
0.4
0.2
0
0
20°
40°
60°
80°
100°
120°
140°
160°
180°
PHASE ANGLE
$H_c = H_g$
$\tau_c = 100$
$A_g = 0.896$
$WS_L = 9.18\ cm^{-1}$
• Isotropic W(0°) = 0.193 cm^{-1}
● Rayleigh W(0°) = 0.179 cm^{-1}
$WS_L = 9.18 \times 10^{-2}\ cm^{-1}$
× Isotropic W(0°) = 0.0156 cm^{-1}
● Rayleigh W(0°) = 0.0143 cm^{-1}
$WS_L = 9.18 \times 10^{-3}\ cm^{-1}$
△ Isotropic W(0°) = $2.23 \times 10^{-3}\ cm^{-1}$
● Rayleigh W(0°) = $2.04 \times 10^{-3}\ cm^{-1}$

Fig. 4

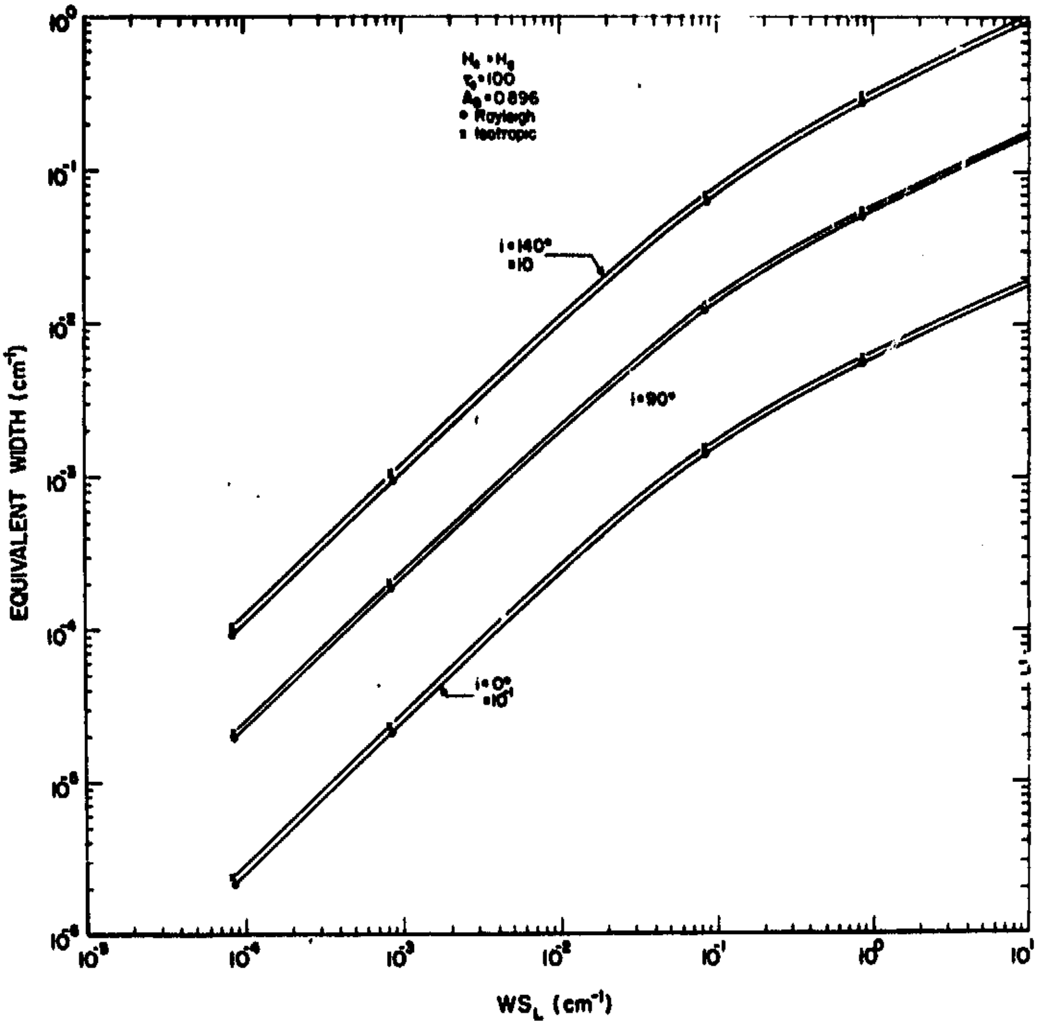

$H_c = H_g$
$\tau_0 = 100$
$A_0 = 0.896$
• Rayleigh
x Isotropic
i = 140°
x10
i = 90°
i = 0°
x10⁻¹
EQUIVALENT WIDTH (cm⁻¹)
WS_L (cm⁻¹)

Fig. 5

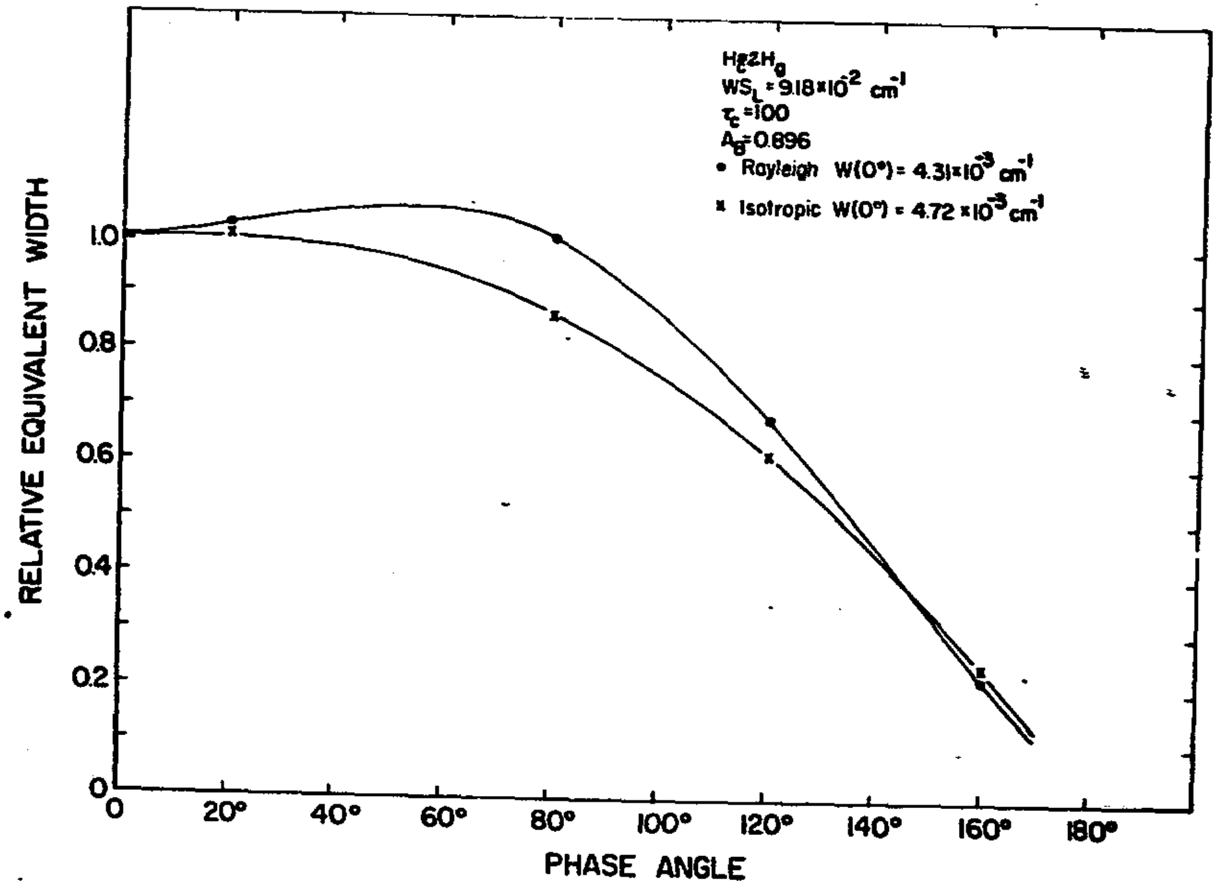
$H_c 2H_g$
$WS_L = 9.18 \times 10^{2}$ cm^{-1}
$\tau_c = 100$
$A_g = 0.896$
• Rayleigh $W(0°) = 4.31 \times 10^{-3}$ cm^{-1}
× Isotropic $W(0°) = 4.72 \times 10^{-3}$ cm^{-1}
RELATIVE EQUIVALENT WIDTH
1.0
0.8
0.6
0.4
0.2
0
0
20°
40°
60°
80°
100°
120°
140°
160°
180°
PHASE ANGLE

Fig. 6

ORIGINAL PAGE IS
OF POOR QUALITY

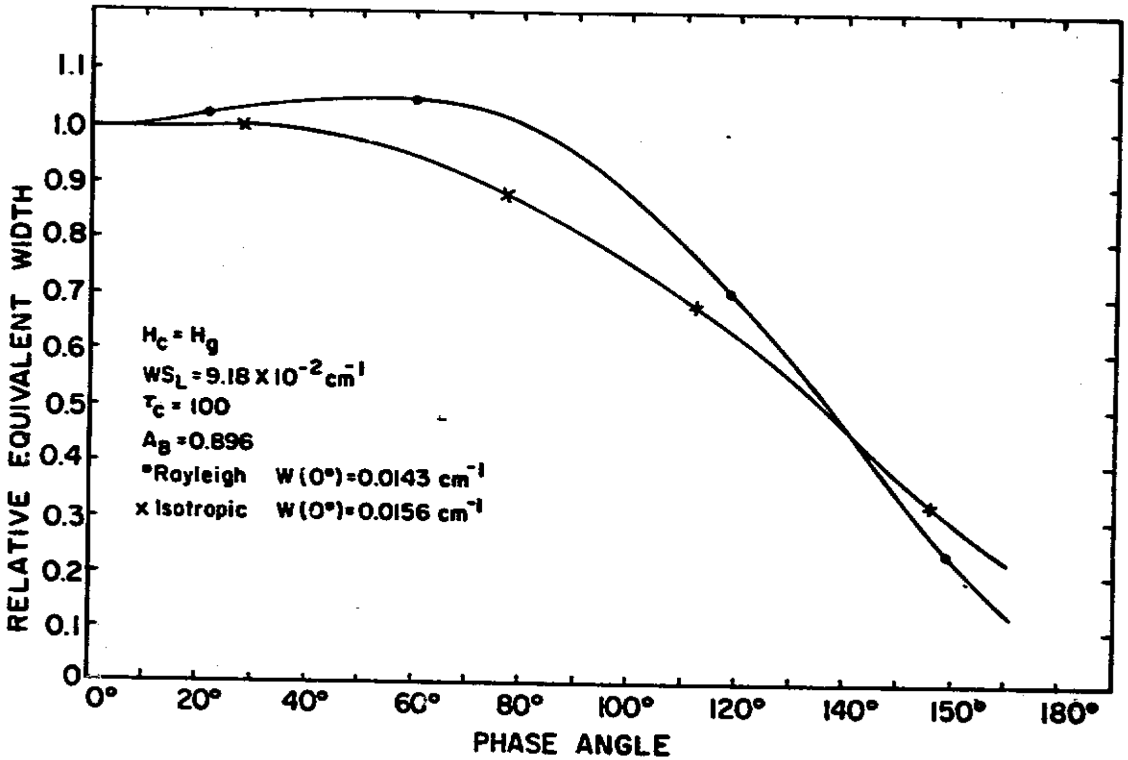

Fig. 7

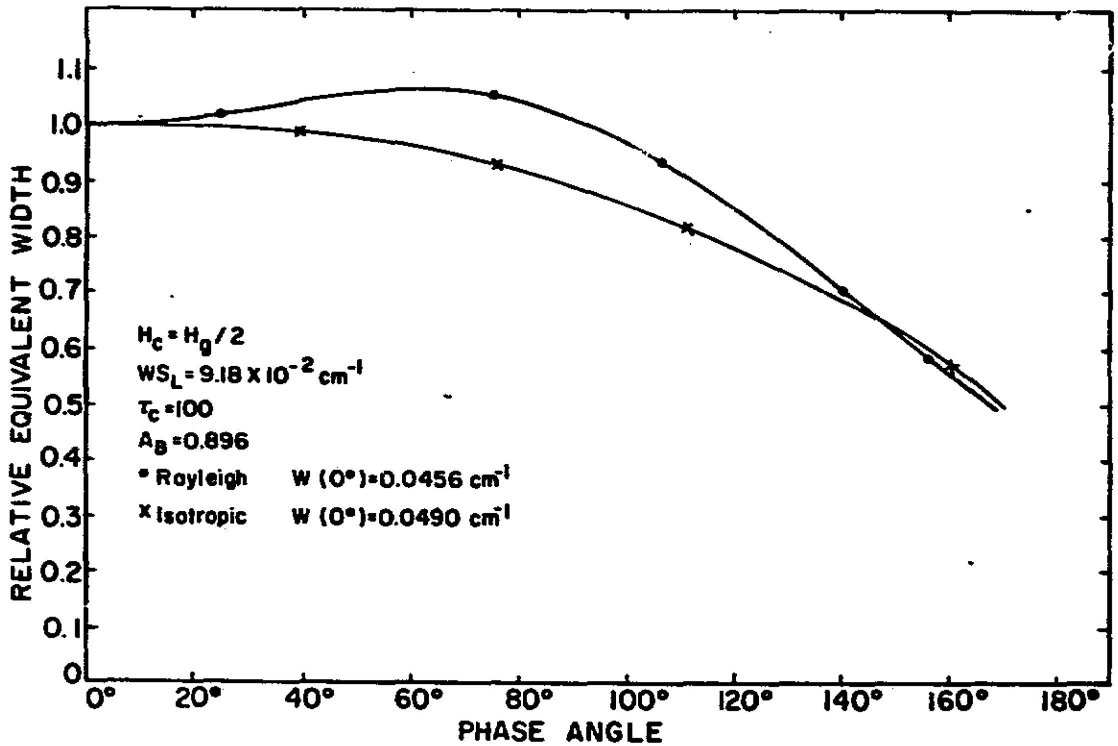
RELATIVE EQUIVALENT WIDTH
1.1
1.0
0.9
0.8
0.7
0.6
0.5
0.4
0.3
0.2
0.1
0
0°
20°
40°
60°
80°
100°
120°
140°
160°
180°
PHASE ANGLE
$H_c = H_g/2$
$WS_L = 9.18 \times 10^{-2}\ cm^{-1}$
$\tau_c = 100$
$A_B = 0.896$
• Rayleigh W (0°) = 0.0456 cm⁻¹
× Isotropic W (0°) = 0.0490 cm⁻¹

Fig. 8

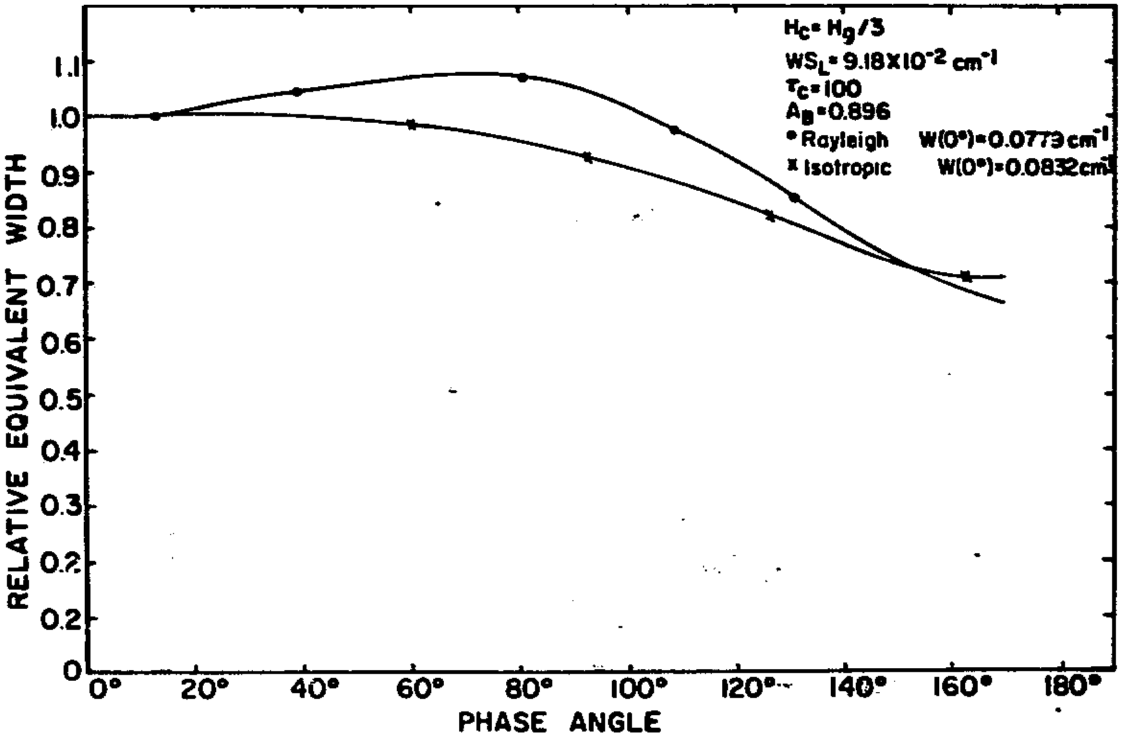

$H_c = H_g/3$
$WS_L = 9.18 \times 10^{-2}$ cm^{-1}
$\tau_c = 100$
$A_B = 0.896$
• Rayleigh W(0°)=0.0773 cm^{-1}
x Isotropic W(0°)=0.0832 cm^{-1}
RELATIVE EQUIVALENT WIDTH
PHASE ANGLE

Fig. 9